

*XVII IMEKO World Congress  
Metrology in the 3rd Millennium  
June 22–27, 2003, Dubrovnik, Croatia*

## DETERMINING MECHANICAL PROPERTIES OF *O1* TOOL STEEL FROM REVERSE COMPUTATION OF INDENTATION MEASUREMENT

*L. Ma, S. Low, J. Song and J. Zhou\**

National Institute of Standards and Technology (NIST), Gaithersburg, MD 20899, USA

\*Department of Mechanical Engineering and Mechanics, Drexel University, Philadelphia, PA 19104, USA

**Abstract** – Besides obtaining the hardness of materials, the indentation test has also been developed as a popular method for investigating mechanical properties. There exist some empirical or semi-analytical methods for determining the hardness, Young's modulus and work hardening exponent from indentation experiments. In this paper, a reverse computation method is introduced to determine the elastic modulus and stress-strain curve of *O1* tool steel from the Rockwell C hardness (HRC) indentation test combined with finite element analysis (FEA) simulation. The force-depth data from the HRC spheroconical indentation measurement is used to start an iterative FEA simulation procedure to extract the elastic-plastic stress-strain relationship which is consistent with the experimentally measured data. The reverse computation results agree well with HRC test results.

**Keywords:** finite element analysis (FEA), indentation, material properties.

### 1. INTRODUCTION

The stress-strain relationship of a material is conventionally obtained from uniaxial tension tests. However, it is difficult to obtain material properties of high hardness specimens, or brittle materials, by uniaxial tension or compression tests. With the growing need of measuring mechanical properties of different materials with small sized specimens or on thin film surfaces, indentation testing is becoming a popular method for investigating the mechanical properties of materials, such as Young's modulus, yield stress, and work-hardening exponent. It has been proposed to determine hardness and elastic modulus values from the initial slope of the unloading curve at the peak load point [1-4]. Recently, several empirical or semi-analytical methods have been proposed to determine the yield stress and stress-strain work hardening exponent from the indentation load-depth curve, in which an finite element analysis (FEA) method is used to extract the mechanical properties of materials by matching the simulated loading and unloading curves with those of the experimentally determined ones [5-10]. Zhao [11] developed an integrated approach combining micro-plane-strain compression testing and FEA simulation, and applied it to determine the elastic-plastic stress-strain relation of polymeric thin films. Ma [12] extended this

method for the simulation of Rockwell indentation of hard materials.

In this paper, base on the HRC spheroconical indentation test and relative FEA model, a reverse computation method is introduced to determine the elastic modulus and stress-strain curve of *O1* tool steel. The reverse computation results are discussed and compared with actual HRC test results, which show good agreement.

### 2. SPHEROCONICAL INDENTATION TEST

To obtain the mechanical properties of NIST standard HRC reference blocks made of *O1* tool steel [13], the following Rockwell indentation experiments were made at NIST. The indenter is a Rockwell diamond indenter which is conical with a spherical tip having a  $120^\circ$  cone angle and  $200\ \mu\text{m}$  tip radius. The indentation force  $L$  (see Fig. 1) was loaded from 0 N to 1471 N using very low penetration velocity ( $1\ \mu\text{m/s}$ ) to decrease the strain rate effect, then unloaded after a short holding time ( $\approx 2\ \text{s}$ ) at maximum force to reduce the effect of material creep. Two test blocks at different nominal hardness levels (45 HRC and 64 HRC) were tested. These tests were performed with the NIST standardizing Rockwell hardness machine at room temperature. The experimental load-depth relationship, combined with the FEA simulation and reverse computation, was used to determine the mechanical properties of the test block. (Note: The HRC measurements

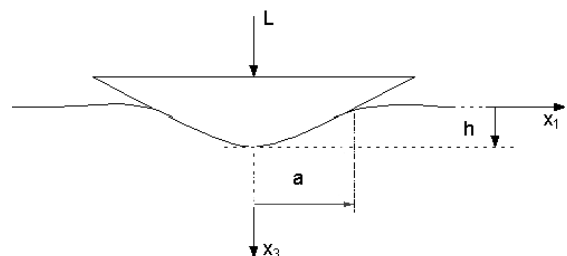


Fig. 1. Schematic of the indenter indenting a half-space. discussed in this paper did not follow a standard Rockwell hardness testing cycle. Therefore, the uncertainty of the HRC values cannot be determined, and should only be evaluated in terms of force and depth measurement uncertainty. All depth measurements reported in this paper are estimated to have an expanded uncertainty no larger than

±0,0001 mm, and all force measurements are estimated to have an expanded uncertainty no larger than ±1 N ( $U = 2u_c$  where  $U$  is the combined uncertainty and  $u_c$  is the combined standard uncertainty).

### 3. FINITE ELEMENT ANALYSIS OF SPHEROCONICAL INDENTATION TESTS

Finite element simulation is tantamount to performing a virtual laboratory test. A finite element model is constructed to computationally simulate the spheroconical indentation experiment. With the advantage of axial symmetry of both the spheroconical indenter and the specimen, only one radial-axial plane is modeled that significantly reduced the complexity of the simulation, and largely improved the simulation efficiency. The Rockwell diamond indenter is modelled as a rigid body. A set of FEA meshes is constructed with an arrangement of quadrilateral, four-node axisymmetric elements. Figure 2 shows the finite element model mesh and boundary conditions. Details of the FEA model are described in reference 12.

### 4. REVERSE COMPUTATION METHOD TO OBTAIN THE STRESS-STRAIN RELATION

Since the indentation load depth curve depends directly on the plastic properties of the indented material, it is possible to determine the constitutive properties from the indentation data. Tabor [1] successfully constructed stress-strain relations using experimental data obtained by spherical indentation in term of the true stress  $\sigma$  and the true plastic strain  $\varepsilon$  as

$$\sigma = \frac{P_t}{3\pi a^2} \quad (1)$$

and

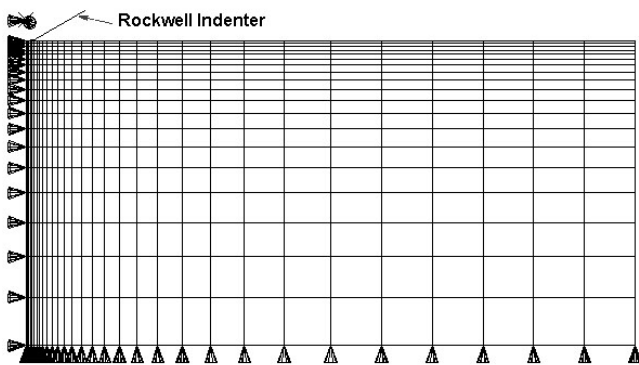


Fig. 2. Finite element model mesh and boundary conditions.

$$\varepsilon = 0,2 \frac{a}{R} \quad (2)$$

respectively, where  $P_t$  is the maximum load,  $R$  is the radius of the indenter, and  $a$  denotes the contact radius. However, this relation is only for a “fully” plastic deformation. Some

researchers [3-9] use the parameter study to obtain the Young’s modulus and hardening response. To fit the force depth curve from the experiment, a large number of FEA iterations must be run.

To enable a more efficient computational analysis, a new reverse computation method is introduced to generate the true stress-strain curve that is consistent with experimental force-displacement data. The basic concept is to use the force-depth data from the indentation test to start an iterative finite element simulation procedure to extract the elastic-plastic stress-strain relationship. The true stress-strain relationship is obtained from the reverse computation method in the following steps.

- (1) Derive the initial approximate material strain hardening properties from the experimental indentation force-displacement relation. The initial approximate indentation stress  $\sigma$  is calculated as the mean pressure under the indenter as

$$\sigma = \frac{L}{\pi a^2} \quad (3)$$

where  $L$  is the indentation force and  $a$  is the ideal maximum contact radius (see Fig. 1) which can be calculated from the indenter’s geometry

$$a = \begin{cases} \sqrt{0,4h - h^2}, & h \leq 0,0268 \text{ mm} \\ 0,1 + (h - 0,0268) \cot 30^\circ, & h > 0,0268 \text{ mm} \end{cases} \quad (4)$$

where  $h$  is the indentation penetration depth. The initial approximate strain  $\varepsilon$  is derived from

$$\varepsilon = \frac{h}{D} \quad (5)$$

where  $D$  is one of the geometrical constants of the spheroconical indenter related to the indenter’s cone angle and tip radius. For the HRC diamond indenter with a 200  $\mu\text{m}$  tip radius and 120° cone angle, when  $D$  is selected as 1982  $\mu\text{m}$ , a minimum deviation, about 4%, relative to the ideal shape of the Rockwell indenter could be achieved [12]. The initial approximate Young’s modulus  $E$  is obtained from the unloading curve as

$$E = \frac{\sigma_{peak} - \sigma_{unload}}{\varepsilon_{peak} - \varepsilon_{unload}} = \frac{D(L_{peak} a_{unload}^2 - L_{unload} a_{peak}^2)}{\pi(h_{peak} - h_{unload})} \quad (6)$$

where the subscripts *peak* and *unload* denote the quantities with the peak force point and first unload point. As the total strain  $\varepsilon$  includes both the elastic strain  $\varepsilon_e$  and plastic strain  $\varepsilon_p$ ,

$$\varepsilon = \varepsilon_e + \varepsilon_p \quad (7)$$

where

$$\varepsilon_e = \frac{\sigma}{E} \tag{8}$$

so the plastic strain  $\varepsilon_p$  can be obtained from

$$\varepsilon_p = \varepsilon - \frac{\sigma}{E}. \tag{9}$$

Now the initial Young's modulus  $E$  and true stress-plastic strain are used as the initial material properties for the initial input of FEA model.

- (2) Conduct a FEA simulation of the Rockwell hardness test using the approximate Young's modulus and stress-plastic strain relation (Eqs. 3, 5, 9) as material properties in the static FEA model.
- (3) Compare the force-displacement curve of FEA simulation with that of actual Rockwell indentation experiments during the loading process. For each indentation force  $L$ , calculate the ratio of indentation penetration depth,  $h_{FEA}/h_{exp}$ . From the difference at each of the compared points along the force-displacement curve, calculate the updating factor from

$$K^i(j) = \frac{h_{FEA}(j)}{h_{exp}(j)}, (j = 1, 2, \dots, n) \tag{10}$$

where the subscript  $FEA$  denotes FEA results and the subscript  $exp$  denotes experiment data. The dummy index  $i$  denotes the current iteration number ( $i = 1$  for the first FEA simulation using the initial approximation of stress-strain relationship), the dummy index  $j$  denotes the sampling points along the force-displacement curve and  $n$  is the total number of compared points. Linear interpolation is used if a FEA sampling point  $j$  for the force-displacement curve does not coincide with a data point from the experimental data points.

Then use the updating factor to update the stress by

$$\sigma^{i+1}(j) = K^i(j)\sigma^i(j). \tag{11}$$

If the updated stress is obtained from the direct point-to-point adjustments, the stress-strain curve becomes serrated because of the non-smooth data from the experimental and FEA results. This is physically unreasonable and computationally troublesome. Therefore, the updating factor points are fit with a smooth curve and substituted to update the stress.

- (4) Perform a new FEA simulation using updated stress-strain relationship as material-properties input. Repeat step (3) until the FEA force-displacement curve sufficiently matches the experimental one.

### 5. RESULTS AND DISCUSSION

Using the above method, the strain-hardening curve with the penetration velocity of  $1\mu\text{m/s}$  for the 45 HRC and 64

HRC blocks are obtained. Figures 3-5 show the comparisons of force-displacement, updating factor and stress-plastic strain for the 45 HRC block. Following the step-by-step procedures, five FEA simulations have been performed to obtain the matched stress-strain relationship. The HRC results from the FEA simulation using the material properties from the FEA reverse computation are very close to the experimental results. For the 45 HRC block, the difference between the FEA and experimental data is 0,133 HRC, and for the 64 HRC block, the difference is 0,166 HRC.

From Fig. 4, it can be seen that the indentation depth ratio between the FEA reverse computation depth and experiment depth varies between 0,45 and 0,55 for the first FEA simulation. After each simulation, the ratio is continually improved until the fifth simulation where the ratio becomes very close to 1 (see Fig. 4). From Fig. 5, it can be seen that the initial stress is about 2,8 to 4 times the FEA matched final stress. It is clear that semi-experimental

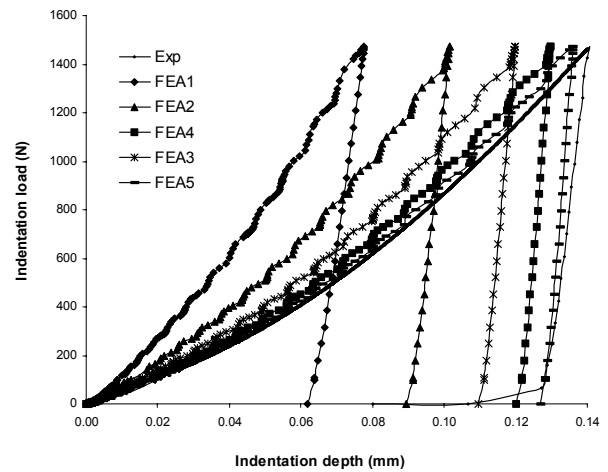


Fig. 3. Comparison of force-displacement curves for the 45 HRC block.

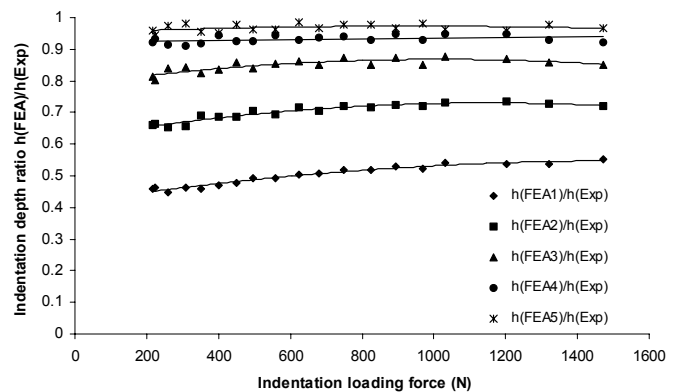


Fig. 4. Comparison of indentation depth ratio for the 45 HRC block.

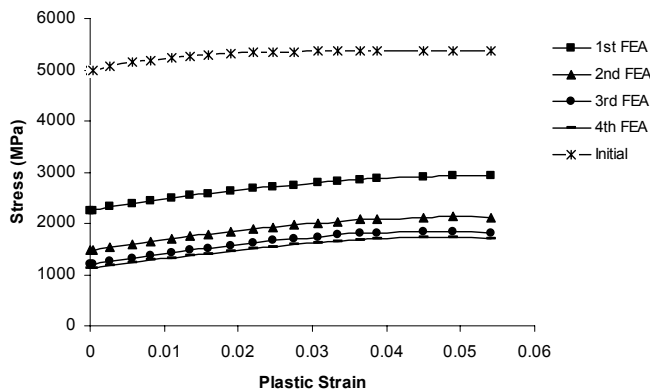


Fig. 5. Comparison of stress-plastic strain curves for the 45 HRC block.

stress and strain (or initial stress strain shown in this paper) cannot represent the material properties.

From Fig. 3 and 4, it can be seen that the improvement for the force-depth curve occurs after each FEA simulation, and the most significant improvement happens between the first and the second FEA simulations. After that, the FEA simulation values become closer to the experimental measurement. This particularly matches for the loading portion (see Fig. 3). Unlike the loading curves, the unloading force-depth curves match only at the initial part of the unloading curve. As unloading progresses, the recover shown on the FEA curve is less than that of the experiment. The tendency of the mismatch on the unloading curve is similar to that observed by Bhattacharya et al. [2] and Zhao [11]. This may be caused by the assumption of the rigid indenter modelled in the FEA model that ignored the indenter elastic deformation during the indentation process. This deformation can also happen at the contact area between the diamond and the holder of the Rockwell indenter. In addition, the FEA model is based on simulating material resistance for continuum material, complex computing mechanisms of stress release may occur in the material during the experiment. More study is needed on what actually happens in the material during the unloading portion of the force-displacement curves. The reverse iteration method needs to be improved by considering these other effects.

## 6. CONCLUSION

The HRC spheroconical indentation tests and relative FEA simulation model for determining the mechanical properties of *OI* steel are described. The reverse computation method is used to determine the elastic modulus and stress-strain curve of *OI* tool steel from the HRC indentation tests combined with the FEA simulation. The force-depth data from the Rockwell spheroconical indentation measurement are used to start an iterative FEA simulation procedure to extract the elastic-plastic stress-strain relationship that is consistent with the experimentally measured data. The reverse computation results are compared with the HRC test results, and show good agreement. Detailed results can be found in Ref. 12.

## REFERENCES

- [1] D. Tabor, "The hardness of Metal", Clarendon Press, Oxford, 1951.
- [2] A. K. Bhattacharya, W. D. Nix, "Analysis of Elastic and Plastic Deformation Associated with Indentation Testing of Thin Films on Substrates", *International Journal of Solids and Structures*, vol. 24, pp. 1287-1298, 1988.
- [3] W. C. Oliver, G. M. Pharr, "An Improved Technique for Determining Hardness and Elastic Modulus Using Load and Displacement Sensing Indentation Experiments," *Journal of Material Research*, vol. 7, no. 6, pp. 1564-1583, 1992.
- [4] J. S. Field, M. V. Swain, "Determining the Mechanical Properties of Small Volumes of Material from Submicrometer Spherical Indentation," *Journal of Material Research*, vol. 10, no. 1, pp. 101-102, 1995.
- [5] K. Zeng, E. Soderlund, A. E. Giannakopoulos, D. J. Rowcliffe, "Controlled Indentation: A General Approach to Determine Mechanical Properties of Brittle Materials," *Acta Mater.*, vol. 44, no.3, pp. 1127-1141, 1996.
- [6] D. Ma, K. Xu, J. He, "Numerical Simulation for Measuring Yield Strength of Thin Metal Film by Nanoindentation Method," *Trans. Nonferrous Met. Soc. China*, vol. 7, no. 3, pp. 65-68, 1997.
- [7] D. Ma, K. Xu, J. He, "A New Method on Evaluating the Yield Strength of Metal Films Using Depth-Sensing Indentation Instrument," *Acta Metallurgica Sinica*, vol. 34, no. 6, pp. 661-666, 1998.
- [8] B. Taljat, T. Zacharia, F. Kosel, "New Analytical Procedure to Determine Stress-Strain Curve from Spherical Indentation Data," *International Journal of Solids and Structures*, vol. 35, no. 33, pp. 4411-4426, 1998.
- [9] S. Jayaraman, G. T. Hahn, W.C. Oliver, C. A. Rubin, P. C. Bastias, "Determination of Monotonic Stress-Strain Curve of Hard Materials from Ultra-Low-Load Indentation Tests," *International Journal of Solids and Structures*, vol. 35 no. 5-6, pp. 365-381, 1998.
- [10] N. Huber, I. Tsagrakis, C. Tsakmakis, "Determination of Constitutive Properties of Thin Metallic Films on Substrates by Spherical Indentation Using Neural Networks," *International Journal of Solids and Structures*, vol. 37, pp. 6499-6516, 2000.
- [11] F. Z. Zhao, "Modeling of Mechanical Behavior of thin films," *Ph.D. thesis, Drexel University*, 1998.
- [12] L. Ma, "Modeling, Simulation and Prediction for Rockwell Hardness Indentation," *Ph.D. thesis, Drexel University*, pp. 119-127, 2001.
- [13] T. Lyman, "Metal Handbook", ASM, vol. 1, pp. 637-654, 1961.

**Authors:** Dr. Li Ma, Guest Researcher, National Institute of Standards and Technology (NIST), Stop 8553, 100 Bureau Drive, Gaithersburg, MD 20899. Tel: 1-301-975-2057, Fax: 1-301-975-4553, Email: li.ma@nist.gov.  
 Sam Low, Materials Research Engineer, NIST, Stop 8553, 100 Bureau Drive, Gaithersburg, MD 20899. Tel: 1-301-975-5709, Fax: 1-301-975-4553, Email: samuel.low@nist.gov.  
 John Song, Mechanical Engineer, NIST, Stop 8212, 100 Bureau Drive, Gaithersburg, MD 20899. Tel: 1-301-975-3799, Fax: 1-301-975-0822, Email: song@nist.gov.  
 Jack Zhou, Associate Professor, Department of Mechanical Engineering and Mechanics, Drexel University, 3141 Chestnut St., Philadelphia, PA 19104. Tel: 1-215-895-1480, Fax: 1-215-895-1478, Email: zhoug@drexel.edu.